Langmuir

Article

pubs.acs.org/Langmuir

Electrostatic-Interaction-Induced Molecular Deposition of a Hybrid Bilayer on Au(111): A Scanning Tunneling Microscopy Study

Jing-Ying Gu,[†,‡] Ting Chen,[†] Lin Wang,[†,‡] Wei-Long Dong,[†,‡] Hui-Juan Yan,[†] Dong Wang,*[,†] and Li-Jun Wan*[,†]

[†]CAS Key Laboratory of Molecular Nanostructure and Nanotechnology and Beijing National Laboratory for Molecular Sciences, Institute of Chemistry, Chinese Academy of Sciences (CAS), Beijing 100190, People's Republic of China

[‡]University of Chinese Academy of Sciences, Beijing 100049, People's Republic of China

Supporting Information

ABSTRACT: Hybrid bilayers consisting of 8-hydroxypyrene-1,3,6-trisulfonic acid trisodium salt (HPTS) and *meso*-tetra(4-pyridyl)porphine (TPyP) have been successfully constructed on Au(111) and investigated by electrochemical scanning tunneling microscopy (ECSTM). Under the guidance of the electrostatic interaction between negatively charged sulfonate groups and positively charged pyridyl groups, the underlying HPTS arrays act as templates for the deposition of cationic TPyPs, forming two types of TPyP/HPTS complex bilayers. The present work provides a feasible way to fabricate hybrid multilayers on the electrode surface via electrostatic interaction, which has great significance for the design of molecular nanodevices.

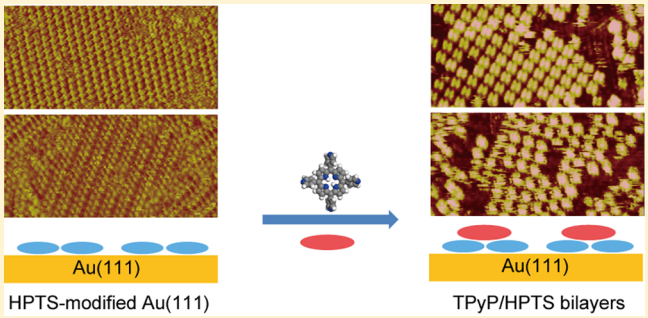

INTRODUCTION

The fabrication of well-defined functional molecular nanostructures on solid surfaces, such as molecular rectifiers,[1,2] molecular nanowires,[3−5] and molecular switches,[6] is one of the crucial steps in the development of molecular nanodevices. Self-assembly is an increasingly used bottom-up strategy for achieving the controllable construction of surface molecular nanostructures.[7,8] The tailored construction of nanoarchitectures of organic molecules on solid surfaces with defined patterns in two dimensions has been successfully demonstrated in a wide variety of systems.[9−13] However, effective methodologies, such as layer-by-layer assembly, Langmuir−Blodgett film construction, and molecular layer deposition, have been developed to obtain thin organic films with ordered structures in the vertical direction.[14−17]

Recently, the fabrication of a hierarchical molecular structure with simultaneous control over in-plane and vertical orderliness has attracted a great amount of attention for surface molecular engineering.[18−25] For example, the direct assembly of ordered arrays of molecular junctions with molecular donors and acceptors is desirable for molecular memory devices and may provide interesting model systems for understanding the electron and charge-transfer process in organic electronics on the molecular level.[18,19,26] In addition, understanding the molecular mechanism for the hybrid molecular bilayer array is closely related to the bulk crystallization process. The supramolecular architectures of hybrid organic bilayers can be assembled through donor−acceptor interaction,[19,22] $\pi-\pi$ interactions,[24,25] coordinative bonds,[27] and hydrogen bonding[28,29] between the molecules of the upper layer and underlayer. For example, Itaya's group reported the construction of a supramolecular assembly consisting of an open-cage fullerene derivative and zinc(II) octaethylporphyrin [Zn(oep)] through donor−acceptor interactions.[19] Effective control over the location and orientation of the upper open fullerene layer by the underlying [Zn(oep)] adlayer results in a well-defined redox process.[19] The surface-supported corannulene-C_{60} host−guest complex bilayer has been tailored by the convex−concave $\pi-\pi$ interaction.[24] Huang et al. demonstrated the preferential adsorption of second-layer F_{16}CuPc on 2D binary supramolecular networks of F_{16}CuPc with other coadsorbers on graphite.[25] In most of these examples, the formation of hybrid bilayer structures is driven by the interactions between the aromatic cores of the molecules. From the viewpoint of surface molecular engineering, it is desirable to establish supramolecular synthons that can be attached to the functional moieties and act as structural directional groups for bilayer formation.

Porphyrins are promising candidates for the fabrication of molecular devices because of their remarkable optical and electronic properties.[30,31] The hybrid bilayer containing porphyrins and other organic molecules is of great interest for molecular devices. In the present work, *meso*-tetra(4-pyridyl)porphine (TPyP) and 8-hydroxypyrene-1,3,6-trisulfonic acid trisodium salt (HPTS) have been chosen as components in

Received: March 5, 2014
Published: March 11, 2014

 © 2014 American Chemical Society dx.doi.org/10.1021/la500873y | *Langmuir* 2014, 30, 3502−3506

the fabrication of ordered hybrid bilayers. The chemical structures of HPTS and TPyP are shown in Figure 1. In acidic

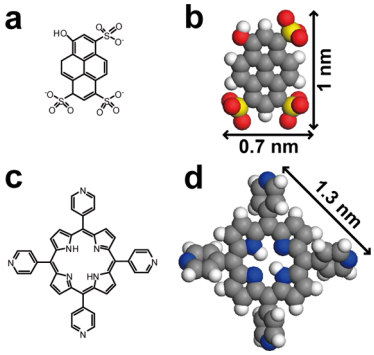

Figure 1. Chemical structures and optimized models of HPTS (a, b) and TPyP (c, d).

solution (0.1 M $HClO_4$), the HPTS molecule is negatively charged because of the deprotonation of the sulfonate groups whereas the TPyP molecule is positively charged because of the protonation of the porphyrin core and pyridyl groups. In situ scanning tunneling microscopy (STM) results indicate that the negatively charged HPTS arrays can act as templates to capture cationic porphyrins via electrostatic interaction, leading to TPyP/HPTS supramolecular bilayer assembly. These results indicate that the pyridyl/sulfonate pair could act as effective supramolecular synthons for the design and construction of hybrid bilayer nanostructures.

EXPERIMENTAL SECTION

8-Hydroxypyrene-1,3,6-trisulfonic acid trisodium salt (HPTS) was purchased from Sigma-Aldrich. *meso*-Tetra(4-pyridyl)porphine (TPyP) was obtained from Frontier Scientific Inc. Both HPTS and TPyP were used without further purification. Electrolyte solution (0.1 M $HClO_4$) was prepared by diluting ultrapure $HClO_4$ (Kanto Chemical Co.) with Milli-Q water (18.2 MΩ·cm, total organic carbon <5 ppb). The Au(111) single-crystal electrode was obtained by the Clavilier method[34] and used as a substrate. Before each experiment, the substrate was annealed in a hydrogen—oxygen flame and cooled in an ultrapure N_2 atmosphere. The HPTS adlayer was formed by immersing the gold bead in a ca. 4 mM HPTS aqueous solution for about 30 s. Then, TPyP/HPTS bilayers were prepared by adding 5 μL of a saturated TPyP solution to the electrochemical cell after the ordered monlayer of HPTS was observed by ECSTM. Electrochemical STM experiments were carried out in 0.1 M $HClO_4$ with a NanoScope E scanning tunneling microscope (Bruker Inc.). A homemade Teflon cell equipped with two Pt wires that served as a reference electrode and counter electrode was used as an electrochemical cell. STM tips were W wires (0.25 mm diameter) that were electrochemically etched in 0.6 M KOH at 12−15 V (ac) and coated with transparent nail polish to minimize the residual faradaic current. All of the STM images were recorded in constant-current mode with a high-resolution scanner and without further processing. All electrode potentials were reported with respect to the RHE in 0.1 M $HClO_4$.

RESULTS AND DISCUSSION

Figure 2a,c represents high-resolution STM images of two typical HPTS adstructures on Au(111) in 0.1 M $HClO_4$. Each HPTS molecule can be resolved as an ellipse. The major axis and the minor axis of the ellipse are measured to be 1.0 and 0.7 nm, respectively, close to the dimension of the HPTS molecule, indicating that the HPTS molecule lies flat on the Au(111) surface.

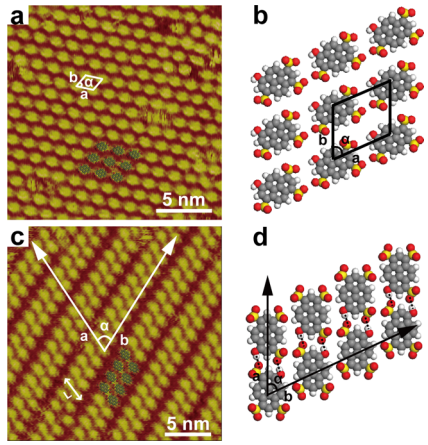

Figure 2. (a, b) High-resolution STM images and proposed structural model of HPTS adstructure (I) on the Au(111) surface. (c, d) High-resolution STM images and proposed structural model of the HPTS adstructure (II) on the Au(111) surface. Image conditions: (a) E = 550 mV, E_{bias} = −515.2 mV, and I_t = 1.251 nA; (c) E = 750 mV, E_{bias} = −380.0 mV, and I_t = 0.690 nA.

Figure 2a displays the close-packed adstructure (I) of HPTS. A rhomboid unit cell is overlaid on the STM image by a white box. The major axis of HPTS molecules is aligned with direction a of the unit cell. The unit cell parameters are measured to be a = 1.4 ± 0.1 nm, b = 1.1 ± 0.1 nm, and α = 68 ± 5°. On the basis of the high-resolution STM image, a tentative structural model for the HPTS adsturcture (I) is proposed in Figure 2b. No obvious directional intermolecular interaction exists in the adlayer.

The stripelike structure is another common structure of the HPTS adlayer, as shown in Figure 2c. The neighboring molecules gather together to form a dimer as the basic unit of the adlayer via intermolecular hydrogen bonds. The width L of each row extracted from the image is ca. 2.2 nm. The dimers arrange into a long-range-ordered stripe structure (direction b, Figure 2c). The distance between neighboring HPTS molecules within the molecular row is ca. 1.0 nm, which is similar to that in the close-packed adstructure (I). However, the stripelike structure of HPTS is disordered in the transverse direction of the molecular stripes as a result of the dislocations between molecular rows. The angle between the molecular major axis (a, Figure 2c) and the molecular alignment row direction (b, Figure 2c) is 65 ± 5°. On the basis of the above structural analysis, a tentative structural model for the HPTS adsturcture (II) is proposed in Figure 3d. The HPTS molecules are preferentially paired in a head-to-head configuration. The O−H···O hydrogen bonds exist between the hydroxyl group and the sulfonate group, as marked by black dashed lines in Figure

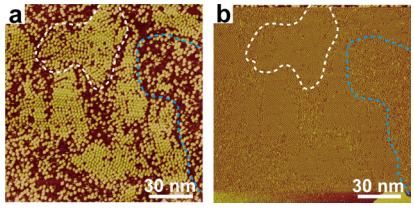

Figure 3. Sequential STM images of TPyP on the HPTS-modified Au(111) surface. Image conditions: (a) E = 550 mV, E_{bias} = −850.0 mV, I_t = 1.816 nA, and data scale = 1.0 nm; (b) E = 550 mV, E_{bias} = −150.0 mV, I_t = 1.816 nA, and data scale = 1.0 nm.

dx.doi.org/10.1021/la500873y | *Langmuir* 2014, 30, 3502−3506

3d. Obviously, the intermolecular hydrogen bonds play an important role in the formation of the HPTS dimer.

After the ordered monolayer of HPTS was observed by ECSTM, 5 μL of a saturated solution of TPyP was directly injected into the electrochemical cell under potential control. About half an hour later, STM imaging was resumed to record the adlayer structure. Figure 3a,b shows sequential STM images of TPyP on the HPTS-modified Au(111) surface, acquired at 550 mV in 0.1 M $HClO_4$ with different imaging parameters. Both the structures of the top layer and underlayer can be resolved with appropriate imaging parameters. When decreasing the bias voltage, that is, extracting the tip from the surface, the top layer of TPyP can be seen, as shown in Figure 3a. Conversely, the underlayer of HPTS can be observed (Figure 3b) when increasing the bias, thus pushing the tip close to the surface. According to the cross-sectional profiles of Figure 3a,b (Figure S1 in the Supporting Information), the height of the upper layer is measured to be ~0.4 nm for the specified imaging parameters, which is significantly greater than the typical apparent height (~0.1 nm) of a porphyrin molecule in the STM image (Figure S2 in the Supporting Information).

A careful comparison of images a and b in Figure 3 reveals that the adsorption structure of TPyP strongly depends on the underlying structure of HPTS. When the underlying HPTS molecules arrange into an ordered structure on Au(111), the top layer of TPyP can adsorb directly on the HPTS adlayer in an ordered form, as indicated by the white dashed lines in Figure 3a,b and the high surface coverage of TPyP on the ordered HPTS adlayer. On the contrary, when the underlying HPTS molecules adsorb on the Au(111) surface in a disordered form, the top layer of TPyP adsorbs randomly on the HPTS adlayer, as illustrated by the blue dashed lines in Figure 3a,b and the low surface coverage of TPyP on the disordered HPTS adlayer. The preferential adsorption of TPyP on the ordered HPTS adlayers encourages us to investigate the epitaxial relationship between the TPyP upper layer and HPTS underlayer.

Figure 4a presents a high-resolution STM image of the top layer of TPyP molecules on the HPTS-modified Au(111) surface, indicating that the TPyP molecules can self-organize into an ordered quadrilateral pattern on the HPTS-modified Au(111) electrode. Different from the hollow square appearance of the TPyP molecule on Au(111) (Figure S2 in the Supporting Information), each TPyP molecule can be identified as a bright square composed of two oblong protrusions. The molecular shape observed in the STM image corresponds to the nonplanar or saddle-shaped conformation of porphyrins as reported previously,[32,33] suggesting that the adsorption of TPyP on the HPTS-modified Au(111) surface induces a strong distortion of TPyP. The reason for the strikingly different adsorption behavior of TPyP on Au(111) and HPTS-modified Au(111) may be the special registry of TPyP on the HPTS adlayer and/or the strong intermolecular interactions.[32]

The underlying HPTS molecules can be dimly visible in the area without TPyP as illustrated by the white arrow overlaid in the STM image, providing further evidence of the formation of the complex TPyP/HPTS bilayer. Figure 4b displays the underlying structure of HPTS by increasing the bias voltage, indicating that the underlying HPTS molecules form a quadrilateral adstructure (I). By changing the scanning condition in one frame, a composite STM image with a top layer and an underlayer was obtained, as shown in Figure 4c. On the basis of the composite STM image, the epitaxial relationship between the upper layer and the underlayer can be deduced, as outlined by the dashed line in Figure 4c. A tentative structural model for the structure (I) of the TPyP/HPTS bilayer is proposed in Figure 4d. Each TPyP molecule sits at the center of three HPTS molecules, and the surface stoichiometric ratio of TPyP to HPTS is 1:3. A rectangular unit cell is shown in Figure 5d, with parameters of $a = 2.0 \pm 0.1$ nm, $b = 2.2 \pm 0.1$ nm, and $\alpha = 82 \pm 5°$.

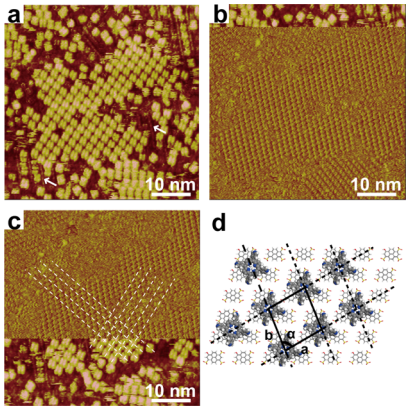

Figure 4. (a–c) Sequential STM images of the TPyP/HPTS bilayer (I) on Au(111). (d) Proposed structural model for the TPyP/HTPS bilayer (I). Imaging conditions: (a) E = 550 mV, E_{bias} = −850.0 mV, and I_t = 1.816 nA. (b) Upper region: E = 550 mV, E_{bias} = −850.0 mV, and I_t = 1.816 nA. Lower region: E = 550 mV, E_{bias} = −150.0 mV, and I_t = 1.816 nA. (c) Upper region: E = 550 mV, E_{bias} = −150.0 mV, and I_t = 1.816 nA. Lower region: E = 550 mV, E_{bias} = −850.0 mV, and I_t = 1.816 nA.

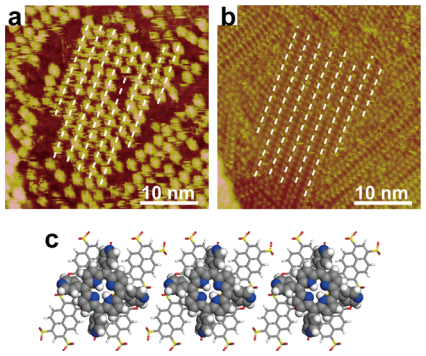

Figure 5. (a, b) Sequential STM images of the TPyP/HPTS bilayer (II) on Au(111). (c) Proposed structural model for the TPyP/HPTS bilayer (II). Imaging conditions: (a) E = 700 mV and E_{bias} = −650.0 mV; (b) E = 700 mV, E_{bias} = −300.0 mV, I_t = 1.000 nA, and I_t = 1.000 nA.

When the arrangement of the underlying HPTS molecules is changed, another type of TPyP/HPTS bilayer can be observed. Figure 5a,b shows typical STM images of the TPyP top layer and the HPTS underlayer, respectively. Eight molecular rows of TPyP have been seen, as illustrated by white dashed lines in Figure 5a that well match the number and length of the HPTS rows in Figure 5b, suggesting that the structure of the top layer depends on the organization of the underlayer. The TPyP molecules adsorb exactly at the center of HPTS rows (Figure 3S in the Supporting Information). The distance between

dx.doi.org/10.1021/la500873y | Langmuir 2014, 30, 3502–3506

neigboring TPyP molecules within molecular rows is 2.0 ± 0.1 nm, which is twice the distance between neigboring HPTS molecules. Meanwhile, the distance between TPyP rows is exactly the same as that between HPTS rows. Moreover, the dislocation between neighboring rows is clearly visible in the TPyP top layer. Therefore, we deduce that each TPyP molecule sits at the center of the quadrangle composed of four HPTS molecules and the surface coverage ratio of TPyP to HPTS is 1:4. On the basis of the above analysis, a tentative structural model is given in Figure 5c.

According to the molecular structures of HPTS and TPyP (Figure 1), there are four kinds of possible molecular interactions: (1) a $\pi-\pi$ interaction between the pyrene ring and porphyrin core, (2) a cation$-\pi$ interaction between the pyrene ring and the positively charged pyridyl group, (3) an electrostatic interaction between the negatively charged sulfonate group and the positively charged porphyrin core, and (4) an electrostatic interaction between the negatively charged sulfonate group and the positively charged pyridyl group. A series of control experiments have been carried out to understand the driving force for the bilayer structure. We find that the adlayers of other conjugated aromatic hydrocarbons (such as perylene and coronene) cannot support the bilayer structure of TPyP or other similar porphyrins, indicating that interactions 1 and 2 are not the primary driving forces for the adsorption of TPyP molecules on HPTS adlayers. In addition, other porphyrin derivatives without pyridyl substituents cannot form a bilayer structure, excluding the effect of interaction 3. Finally, we successfully observe the bilayer structure of a pyridyl-modified porphyrin such as zinc 5,10,15,20-tetra(4-pyridyl)-21*H*,23*H*-porphine (Zn-TPyP) on top of the HPTS-modified Au(111) electrode (Figure S7 in the Supporting Information). This proves that the electrostatic interaction between the negatively charged sulfonate group and the positively charged pyridyl group is the primary driving force for the adsorption of TPyP molecules on HPTS adlayers.

CONCLUSIONS

The bilayer assemblies of TPyP and HPTS at the Au(111)/0.1 M aqueous perchloric acid interface have been studied by ECSTM. It is found that the negatively charged HPTS arrays can act as templates to control the adsorption of positively charged TPyP molecules via electrostatic interaction, forming TPyP/HPTS complex bilayers. Two types of top-layer structures that are epitaxially grown on the underlayer structures have been observed by ECSTM. These kinds of hybrid bilayers may be potentially useful for molecular rectifiers.[1] Furthermore, we demonstrate that the electrostatic interaction between the negatively charged sulfonate group and the positively charged pyridyl group is the primary driving force for the formation of complex TPyP/HPTS bilayers by several control experiments. We expect that the pyridyl/sulfonate supramolecular synthons can be extended to control the bilayer or multilayer dyad array of other functional organic molecules, which is of great significance in the development of molecular nanodevices.

ASSOCIATED CONTENT

Supporting Information

Additional STM results. This material is available free of charge via the Internet at http://pubs.acs.org.

AUTHOR INFORMATION

Corresponding Authors

*E-mail: wangd@iccas.ac.cn.

*E-mail: wanlijun@iccas.ac.cn.

Notes

The authors declare no competing financial interest.

ACKNOWLEDGMENTS

We are thankful for financial support from the National Key Project on Basic Research (grants 2011CB808700 and 2011CB932304), the National Natural Science Foundation of China (grants 21121063, 21073204, 21373236, and 21127901), the Beijing Municipal Education Commission (20118000101), and the Chinese Academy of Sciences.

REFERENCES

(1) Yang, Y. C.; Chang, C. H.; Lee, Y. L. Complexation of fullerenes on a pentacene-modified Au(111) surface. *Chem. Mater.* **2007**, *19*, 6126−6130.

(2) Matino, F.; Arima, V.; Piacenza, M.; Della Sala, F.; Maruccio, G.; Phaneuf, R. J.; Del Sole, R.; Mele, G.; Vasapollo, G.; Gigli, G.; Cingolani, R.; Rinaldi, R. Rectification in supramolecular zinc porphyrin/fulleropyrrolidine dyads self-organized on gold(111). *ChemPhysChem* **2009**, *10*, 2633−2641.

(3) Okawa, Y.; Aono, M. Materials science - nanoscale control of chain polymerization. *Nature* **2001**, *409*, 683−684.

(4) Akai-Kasaya, M.; Shimizu, K.; Watanabe, Y.; Saito, A.; Aono, M.; Kuwahara, Y. Electronic structure of a polydiacetylene nanowire fabricated on highly ordered pyrolytic graphite. *Phys. Rev. Lett.* **2003**, *91*, 25501.

(5) Sakaguchi, H.; Matsumura, H.; Gong, H.; Abouelwafa, A. M. Direct visualization of the formation of single-molecule conjugated copolymers. *Science* **2005**, *310*, 1002−1006.

(6) Lewis, P. A.; Inman, C. E.; Maya, F.; Tour, J. M.; Hutchison, J. E.; Weiss, P. S. Molecular engineering of the polarity and interactions of molecular electronic switches. *J. Am. Chem. Soc.* **2005**, *127*, 17421−17426.

(7) Otero, R.; Gallego, J. M.; de Parga, A. L. V.; Martin, N.; Miranda, R. Molecular self-assembly at solid surfaces. *Adv. Mater.* **2011**, *23*, 5148−5176.

(8) De Feyter, S.; De Schryver, F. C. Self-assembly at the liquid/solid interface: STM reveals. *J. Phys. Chem. B* **2005**, *109*, 4290−4302.

(9) Yuan, Q. H.; Xing, Y. J.; Borguet, E. An STM Study of the pH dependent redox activity of a two-dimensional hydrogen bonding porphyrin network at an electrochemical interface. *J. Am. Chem. Soc.* **2010**, *132*, 5054−5060.

(10) Friesen, B. A.; Wiggins, B.; McHale, J. L.; Mazur, U.; Hipps, K. W. A Self-assembled two-dimensional zwitterionic structure: H6TSPP studied on graphite. *J. Phys. Chem. C* **2011**, *115*, 3990−3999.

(11) Bebensee, F.; Svane, K.; Bombis, C.; Masini, F.; Klyatskaya, S.; Besenbacher, F.; Ruben, M.; Hammer, B.; Linderoth, T. Adsorption and dehydrogenation of tetrahydroxybenzene on Cu(111). *Chem. Commun.* **2013**, *49*, 9308−9310.

(12) Tahara, K.; Inukai, K.; Adisoejoso, J.; Yamaga, H.; Balandina, T.; Blunt, M. O.; De Feyter, S.; Tobe, Y. Tailoring surface-confined nanopores with photoresponsive groups. *Angew. Chem., Int. Ed.* **2013**, *52*, 8373−8376.

(13) Pieta, P.; Mirza, J.; Lipkowski, J. Direct visualization of the alamethicin pore formed in a planar phospholipid matrix. *Proc. Natl. Acad. Sci. U.S.A.* **2012**, *109*, 21223−21227.

(14) Rajesh, K.; Chandra, M. S.; Hirakawa, S.; Kawamata, J.; Radhakrishnan, T. P. Polyelectrolyte templating strategy for the fabrication of multilayer hemicyanine Langmuir-Blodgett films showing enhanced and stable second harmonic generation. *Langmuir* **2007**, *23*, 8560−8568.

(15) Doron-Mor, I.; Cohen, H.; Cohen, S. R.; Popovitz-Biro, R.; Shanzer, A.; Vaskevich, A.; Rubinstein, I. Layer-by-layer assembly of

ordinary and composite coordination multilayers. *Langmuir* **2004**, *20*, 10727−10733.
(16) Schulz, C.; Nowak, S.; Frohlich, R.; Ravoo, B. J. Covalent layer-by-layer assembly of redox active molecular multilayers on silicon (100) by photochemical thiol-ene chemistry. *Small* **2012**, *8*, 569−577.
(17) Lee, B. H.; Yoon, B.; Abdulagatov, A. I.; Hall, R. A.; George, S. M. Growth and properties of hybrid organic-inorganic metalcone films using molecular layer deposition techniques. *Adv. Funct. Mater.* **2013**, *23*, 532−546.
(18) Bonifazi, D.; Spillmann, H.; Kiebele, A.; de Wild, M.; Seiler, P.; Cheng, F. Y.; Guntherodt, H. J.; Jung, T.; Diederich, F. Supramolecular patterned surfaces driven by cooperative assembly of C-60 and porphyrins on metal substrates. *Angew. Chem., Int. Ed.* **2004**, *43*, 4759−4763.
(19) Yoshimoto, S.; Tsutsumi, E.; Honda, Y.; Murata, Y.; Murata, M.; Komatsu, K.; Ito, O.; Itaya, K. Controlled molecular orientation in an adlayer of a supramolecular assembly consisting of an open-cage C-60 derivative and Zn-II octaethylporphyrin on Au(111). *Angew. Chem., Int. Ed.* **2004**, *43*, 3044−3047.
(20) Yoshimoto, S.; Tsutsumi, E.; Fujii, O.; Narita, R.; Itaya, K. Effect of underlying coronene and perylene adlayers for 60 fullerene molecular assembly. *Chem. Commun.* **2005**, 1188−1190.
(21) Mena-Osteritz, E.; Bauerle, P. Complexation of C-60 on a cyclothiophene monolayer template. *Adv. Mater.* **2006**, *18*, 447−451.
(22) Bonifazi, D.; Kiebele, A.; Stohr, M.; Cheng, F. Y.; Jung, T.; Diederich, F.; Spillmann, H. Supramolecular nanostructuring of silver surfaces via self-assembly of [60]fullerene and porphyrin modules. *Adv. Funct. Mater.* **2007**, *17*, 1051−1062.
(23) Yoshimoto, S.; Tsutsumi, E.; Narita, R.; Murata, Y.; Murata, M.; Fujiwara, K.; Komatsu, K.; Ito, O.; Itaya, K. Epitaxial supramolecular assembly of fullerenes formed by using a coronene template on a Au(111) surface in solution. *J. Am. Chem. Soc.* **2007**, *129*, 4366−4376.
(24) Xiao, W.; Passerone, D.; Ruffieux, P.; Ait-Mansour, K.; Groning, O.; Tosatti, E.; Siegel, J. S.; Fasel, R. C-60/corannulene on Cu(110): a surface-supported bistable buckybowl-buckyball host-guest system. *J. Am. Chem. Soc.* **2008**, *130*, 4767−4771.
(25) Huang, Y. L.; Chen, W.; Wee, A. T. S. Molecular trapping on two-dimensional binary supramolecular networks. *J. Am. Chem. Soc.* **2011**, *133*, 820−825.
(26) Wen, R.; Yan, C.-J.; Yan, H.-J.; Pan, G.-B.; Wan, L.-J. Donor/acceptor complex of triphenylene and trinitrotoluene on Au(111): a scanning tunneling microscopy study. *Chem. Commun.* **2011**, *47*, 6915−6917.
(27) Visser, J.; Katsonis, N.; Vicario, J.; Feringa, B. L. Two-dimensional molecular patterning by surface-enhanced zn-porphyrin coordination. *Langmuir* **2009**, *25*, 5980−5985.
(28) Lei, S. B.; Wang, C.; Fan, X. L.; Wan, L. J.; Bai, C. L. Site-selective adsorption of benzoic acid using an assembly of tridodecylamine as the molecular template. *Langmuir* **2003**, *19*, 9759−9763.
(29) Nicholls, D.; McKinzie, W. P.; Oncel, N. 5-(Octadecyloxy) isophthalic acid-assisted copper(II) meso-tetra (4-carboxyphenyl) porphyrin adsorption on highly ordered pyrolytic graphite. *J. Phys. Chem. C* **2010**, *114*, 14983−14985.
(30) Jurow, M.; Schuckman, A. E.; Batteas, J. D.; Drain, C. M. Porphyrins as molecular electronic components of functional devices. *Coord. Chem. Rev.* **2010**, *254*, 2297−2310.
(31) Lindsey, J. S.; Bocian, D. F. Molecules for charge-based information storage. *Acc. Chem. Res.* **2011**, *44*, 638−650.
(32) Auwarter, W.; Klappenberger, F.; Weber-Bargioni, A.; Schiffrin, A.; Strunskus, T.; Woll, C.; Pennec, Y.; Riemann, A.; Barth, J. V. Conformational adaptation and selective adatom capturing of tetrapyridyl-porphyrin molecules on a copper (111) surface. *J. Am. Chem. Soc.* **2007**, *129*, 11279−11285.
(33) Yokoyama, T.; Kamikado, T.; Yokoyama, S.; Mashiko, S. Conformation selective assembly of carboxyphenyl substituted porphyrins on Au (111). *J. Chem. Phys.* **2004**, *121*, 11993−11997.
(34) Clavilier, J.; Faure, R.; Guinet, G.; Durand, R. Preparation of mono-crystalline Pt microelectrodes and electrochemical study of the plane surfaces cut in the direction of the (111) and (110) planes. *J. Electroanal. Chem.* **1980**, *107*, 205−209.